Adsorption Behavior of Linear and Cyclic Genetically Engineered Platinum Binding Peptides

Urartu Ozgur Safak Seker,[†,‡] Brandon Wilson,[†] Sevil Dincer,[†] Il Won Kim,[§] Ersin Emre Oren,[†] John Spencer Evans,[§] Candan Tamerler,*[,†,‡] and Mehmet Sarikaya*[,†]

Genetically Engineered Materials Science and Engineering Center, Materials Science and Engineering, University of Washington, Seattle, Washington 98195, Molecular Biology and Genetics, Istanbul Technical University, Maslak, Istanbul, Turkey, and Laboratory for Chemical Physics, New York University, 345 East 24th Street, New York, New York 10010

Received February 14, 2007. In Final Form: May 10, 2007

Recently, phage and cell-surface display libraries have been adapted for genetically selecting short peptides for a variety of inorganic materials. Despite the enormous number of inorganic-binding peptides reported and their bionanotechnological utility as synthesizers and molecular linkers, there is still a limited understanding of molecular mechanisms of peptide recognition of and binding to solid materials. As part of our goal of genetically designing these peptides, understanding the binding kinetics and thermodynamics, and using the peptides as molecular erectors, in this report we discuss molecular structural constraints imposed upon the quantitative binding characteristics of peptides with an affinity for inorganics. Specifically, we use a high-affinity seven amino acid Pt-binding sequence, PTSTGQA, as we reported in earlier studies and build two constructs: one is a Cys-Cys constrained "loop" sequence (CPTSTGQAC) that mimics the domain used in the pIII tail sequence of the phage library construction, and the second is the linear form, a septapeptide, without the loop. Both sequences were analyzed for their adsorption behavior on Pt thin films by surface plasmon resonance (SPR) spectroscopy and for their conformational properties by circular dichroism (CD). We find that the cyclic peptide of the integral Pt-binding sequence possesses single or 1:1 Langmuir adsorption behavior and displays equilibrium and adsorption rate constants that are significantly larger than those obtained for the linear form. Conversely, the linear form exhibits biexponential Langmuir isotherm behavior with slower and weaker binding. Furthermore, the structure of the cyclic version was found to adopt a random coil molecular conformation, whereas the linear version adopts a polyproline type II conformation in equilibrium with the random coil. The 2,2,2-trifluoroethanol titration experiments indicate that TFE has a different effect on the secondary structures of the linear and cyclic versions of the Pt binding sequence. We conclude that the presence of the Cys-Cys restraint affects both the conformation and binding behavior of the integral Pt-binding septapeptide sequence and that the presence or absence of constraints could be used to tune the adsorption and structural features of inorganic binding peptide sequences.

Introduction

Recently, material-specific bacterial and viral peptide libraries[1,2] have been generated using combinatorial biology techniques such as phage- and cell-surface display.[3−5] Peptide sequences with an affinity toward solid materials such as Au,[3] GaAs,[4] Pt,[5] ZnO,[6,7] $CaCO_3$,[8] CNT[9] (carbon nanotube), Ag,[10] CuO_2,[7] and TiO_2[11] have been characterized using a number of approaches, such as numeric counting of phage or bacterial cell binding,[7] quartz crystal microbalance (QCM),[12] and fluorescence microscopy.[13] In some limited cases, the binding characteristics of these sequences have been explored, and adsorption behavior has been quantified.[14] Material-specific peptide sequences have already found applications as molecular linkers, synthesizers, and morphogenizers in the fields of nanotechnology, bionanotechnology, and molecular medicine where specific surface recognition is a requirement for designing devices such as biosensors and biological assays,[15] synthesis,[16,17]and the oriented assembly of materials.[18−20] Despite recent progress, however, there is a need for additional and more quantitative data regarding the molecular mechanisms that facilitate peptide recognition of and binding on solid materials. In particular, it is desirable to

* Corresponding authors. (C.T.) E-mail: tamerler@itu.edu.tr. Tel: 90 (212) 285-3301. Fax: 90 (212) 285-1896. (M.S.) E-mail: sarikaya@u.washington.edu. Tel: (206) 543-0724. Fax: (206) 543-6381.

† University of Washington.

‡ Istanbul Technical University.

§ New York University.

(1) Smith, G. P. *Science* **1985**, *228*, 1315−1317.

(2) Wittrup, K. D. *Curr. Opin. Biotechnol.* **2001**, *12*, 395−399.

(3) Brown, S. *Nat. Biotechnol.* **1997**, *15*, 269−272.

(4) Whaley, S. R.; English, D. S.; Hu, E. L.; Barbara, P. F.; Belcher, A. M. *Nature* **2000**, *405*, 665−668.

(5) Sarikaya, M.; Tamerler, C.; Jen, A. K. Y.; Schulten, K.; Baneyx, F. *Nat. Mater.* **2003**, *2*, 577−585.

(6) Umetsu, M.; Mizuta, M.; Tsumoto, K.; Ohara, S.; Takami, S.; Watanabe, H.; Kumagai, I.; Adschiri, T. *Adv. Mater.* **2005**, *17*, 2571−2575.

(7) Thai, C. K.; Dai, H. X.; Sastry, M. S. R.; Sarikaya, M.; Schwartz, D. T.; Baneyx, F. *Biotechnol. Bioeng.* **2004**, *87*, 129−137.

(8) Li, C. M.; Botsaris, G. D.; Kaplan, D. L. *Cryst. Growth Des.* **2002**, *2*, 387−393.

(9) Wang, S. Q.; Humphreys, E. S.; Chung, S. Y.; Delduco, D. F.; Lustig, S. R.; Wang, H.; Parker, K. N.; Rizzo, N. W.; Subramoney, S.; Chiang, Y. M.; Jagota, A. *Nat. Mater.* **2003**, *2*, 196−200.

(10) Naik, R. R.; Stringer, S. J.; Agarwal, G.; Jones, S. E.; Stone, M. O. *Nat. Mater.* **2002**, *1*, 169−172.

(11) Sano, K. I.; Sasaki, H.; Shiba, K. *Langmuir* **2005**, *21*, 3090−3095.

(12) Sano, K.; Ajima, K.; Iwahori, K.; Yudasaka, M.; Iijima, S.; Yamashita, I.; Shiba, K. *Small* **2005**, *1*, 826−832.

(13) Sarikaya, M.; Tamerler, C.; Schwartz, D. T.; Baneyx, F. O. *Ann. Rev. Mater. Res.* **2004**, *34*, 373−408.

(14) Hayashi, T.; Sano, K.; Shiba, K.; Kumashiro, Y.; Iwahori, K.; Yamashita, I.; Hara, M. *Nano Lett.* **2006**, *6*, 515−519.

(15) Park, T. J.; Lee, S. Y.; Lee, S. J.; Park, J. P.; Yang, K. S.; Lee, K. B.; Ko, S.; Park, J. B.; Kim, T.; Kim, S. K.; Shin, Y. B.; Chung, B. H.; Ku, S. J.; Kim, D. H.; Choi, I. S. *Anal. Chem.* **2006**, *78*, 7197−7205.

(16) Flynn, C. E.; Mao, C. B.; Hayhurst, A.; Williams, J. L.; Georgiou, G.; Iverson, B.; Belcher, A. M. *J. Mater. Chem.* **2003**, *13*, 2414−2421.

(17) Mao, C. B.; Solis, D. J.; Reiss, B. D.; Kottmann, S. T.; Sweeney, R. Y.; Hayhurst, A.; Georgiou, G.; Iverson, B.; Belcher, A. M. *Science* **2004**, *303*, 213−217.

(18) Mao, C. B.; Flynn, C. E.; Hayhurst, A.; Sweeney, R.; Qi, J. F.; Georgiou, G.; Iverson, B.; Belcher, A. M.; *Proc. Natl. Acad. Sci. U.S.A.* **2003**, *100*, 6946−6951.

(19) Sano, K.; Sasaki, H.; Shiba, K. *J. Am. Chem. Soc.* **2006**, *128*, 1717−1722.

(20) Dai, H. X.; Choe, W. S.; Thai, C. K.; Sarikaya, M.; Traxler, B. A.; Baneyx, F.; Schwartz, D. T. *J. Am. Chem. Soc.* **2005**, *127*, 15637−15643.

10.1021/la700446g CCC: $37.00
Published on Web 06/19/2007

understand how primary (amino acid sequence) and secondary (conformational) structure plays a role in the recognition and binding of these short peptides (7−14 amino acids) to inorganic materials. New research is now beginning to provide design principles in tailoring such peptides, generally termed genetically engineered polypeptides for inorganics (GEPI)).[5] For example, simulation studies of peptide interactions with Pt have provided insight into peptide backbone conformation, side chain/surface interaction, and the contributions of peptide structure to observed binding affinities.[21] Similarly, NMR investigations have been utilized to understand how open, unfolded peptide structures facilitate peptide-catalyzed Au crystal formation as well as peptide−Au surface interactions.[22] A quantitative understanding of molecular mechanisms of binding would be useful in designing robust peptides that not only bind specifically to a given material but also can be "tuned" to recognize surface features at a given interface.

Going beyond gold-binding[3] and silver-binding[10] peptides reported earlier, in this work we used one of the strongly binding peptides for platinum, a technologically and biologically important noble metal. The Pt-binding septapeptides were originally selected by screening an M13 phage library using the minor coat pIII Cys-Cys constrained random septapeptides.[5] Two synthetic peptides were used in this study that represent different molecular constraints of the integral high-affinity 7-AA phage Pt binding sequence, PTSTGQA. These are the original cyclic form (cyclic c-PtBP1 = CPTSTGQAC, disulfide-linked) and a linearized version with the Cys-Cys loop deleted (linear l-PtBP1 = PTSTGQA). By incorporating surface plasmon resonance (SPR) and circular dichroism (CD), we were able to analyze the consequence of the loop constraint on peptide adsorption and kinetics and the conformation of peptides and relate them to each other with a comparative approach. Our work provides a new methodology for studying quantitative peptide-based molecular interactions on a Pt substrate using SPR techniques[23] utilizing a Cr−Au−Pt-coated SPR chip.[24,25] We find that the constrained sequence exhibits higher affinity binding to platinum surfaces that does its linearized form. Moreover, the kinetics of peptide adsorption is different for both forms. A parallel study carried out using CD experiments reveals that the presence of the Cys-Cys loop affects the structure and conformational stability of the Pt binding sequence. Collectively, these results demonstrate that molecular constraints play a critical role in peptide binding to Pt, and this feature could be manipulated to affect the recognition and affinity of short peptide sequences for specific inorganic materials.

Materials and Methods

Phage Display Protocol. The target material (polycrystalline platinum powder) was cleaned using ethanol (95%) and equilibrated using phosphate/carbonate (abbreviated as PC, 55 mM KH_2PO_4, 45 mM Na_2CO_3, 200 mM NaCl, pH 7.4) buffer overnight. After this procedure, a Ph.D.-C7C phage display peptide library kit (New England BioLabs Inc.) containing 1.2×10^9 different randomized peptide sequences is then brought into contact with the Pt material. The samples in the library are incubated with platinum powder in potassium PC buffer containing 0.1% detergent (Tween 20 and Tween 80, Merck). Unbound phages are removed by washing with PC buffer containing 0.1% detergent (Tween 20 and Tween 80, Merck). Specifically bound phages are eluted from the surface using different elution buffers (Supporting Information); the eluted phage pool is amplified with *Eschericia coli* ER2738. Amplified phages are purified and subsequently used for additional panning rounds. After each round, the phages are grown on solid media, and single clones are selected by picking single-phage plaques. DNA of single-phage clones are then isolated and sequenced. Because the insert positions of the random sequences are known, the peptide sequenced displayed on each clone can be obtained from the DNA sequences.

Solid-Phase Synthesis of Model Phage Sequences. The Cys-Cys disulfide loop version of the highest affinity 7-AA phage sequence, cyclic-PtBP1 (CPTSTGQAC), and linear-PtBP1 (PTSTGQA) were synthesized using standard *Fmoc* solid-phase peptide synthesis techniques and purified using C-18 reverse-phase liquid chromatography (RPLC) to a level of >95% (United Biochemical Research). With the exception of the circular dichroism experiments, peptide solutions for SPR measurements were prepared in PC buffer at pH 7.5.

Surface Plasmon Resonance (SPR) Experiments. The SPR measurements were made with a dual-channel instrument (Kretschmann configuration) developed by the Radio Engineering Institute, Czech Republic.[26,27] The instrument was equipped with a polychromatic light source (Ocean Optics LS1) connected to the detector via fiber optic cables. The collimator and detector sensors were placed on two mobile arms, allowing adjustment of the incident angle of the light. The flow cell was constructed from PTFE and was placed on a goniometer, and a Mylar gasket was used to prevent leakage between both channels. The instrument has a threshold of detection at a level of ±0.0001 refractive index unit. The prism and glass slides were both made of BK7 glass with a refractive index (RI) of 1.510, and the substrate coupled with the immersion oil has an RI of 1.510.

Our work here provides a new methodology for studying quantitative peptide based-molecular interactions with platinum substrates. To our knowledge, this is a first in the literature. Unlike Ag and Au, noble metals Pt and Pd do not have measurable SPR signals. To overcome this limitation, we use a very thin layer (a few nanometers thick) of Pt coated on a Au substrate (see below) and probe on the SPR signal from the Au layer, now containing the "adsorbed/deposited" Pt layer as well. (The thickness of the platinum used was predetermined by a model, developed by our group, and has not been published). By this approach, the interaction between a molecule and the Pt substrate could be monitored. In this work, the molecule is a genetically selected Pt-binding peptide, and the model allows us to investigate, in detail, the kinetics of adsorption of the peptides onto the Pt substrate.

We developed an approach to construct SPR chips that possess nanometer thicknesses of platinum coating for our studies (unpublished). Empirically, we found that to obtain a reasonable signal from a molecule bound to a specific target thin film, one must first create a layer of gold or silver beneath the target material. To guide the preparation of the Pt substrate (the target), an SPR model was developed that provided the highest SPR signal at an optimum thicknesses of 2 nm Cr, 33 nm Au, and 2 nm Pt (Figure 1). Bare glass substrates (RI = 1.517, Gentel Biosurfaces, WI) were first sonicated in ethanol and then rinsed with deionized water and dried using high-purity nitrogen gas. To eliminate organic contamination, these slides were then treated with a UV-ozone cleaner for 15 min. The clean glass slides were then coated with Cr, followed by Au and finally Pt (Figure 1), as determined using the quartz crystal microbalance located in the deposition chamber. All of the coatings were generated using an ion beam and a precision etching coater system (Gatan Inc, Pleasanton, CA) operating at 6 keV, 10 mA/cm^2 ion current density, and 6×10^{-5} Torr vacuum. Platinum, chromium, and gold targets of 99.99% purity were purchased from Gatan Inc.

(21) Oren, E. E.; Tamerler, C.; Sarikaya, M. *Nano Lett.* **2005**, *5*, 415−419.
(22) Kulp, J. L.; Sarikaya, M.; Evans, J. S. *J. Mater. Chem.* **2004**, *14*, 2325−2332.
(23) Tamerler, C.; Oren, E. E.; Duman, M.; Venkatasubramanian, E.; Sarikaya, M. *Langmuir* **2006**, *22*, 7712−7718.
(24) Kambhampati, D. K.; Jakob, T. A. M.; Robertson, J. W.; Cai, M.; Pemberton, J. E.; Knoll, W. *Langmuir* **2001**, *17*, 1169−1175.
(25) Szunerits, S.; Boukherroub, R. *Langmuir* **2006**, *22*, 1660−1663.
(26) Homola, J.; Lu, H. B. B.; Nenninger, G. G.; Dostalek, J.; Yee, S. S. *Sens. Actuators, B* **2001**, *76*, 403−410.
(27) Zhu, X. M.; Lin, P. H.; Ao, P.; Sorensen, L. B. *Sens. Actuators, B* **2002**, *84*, 106−112.

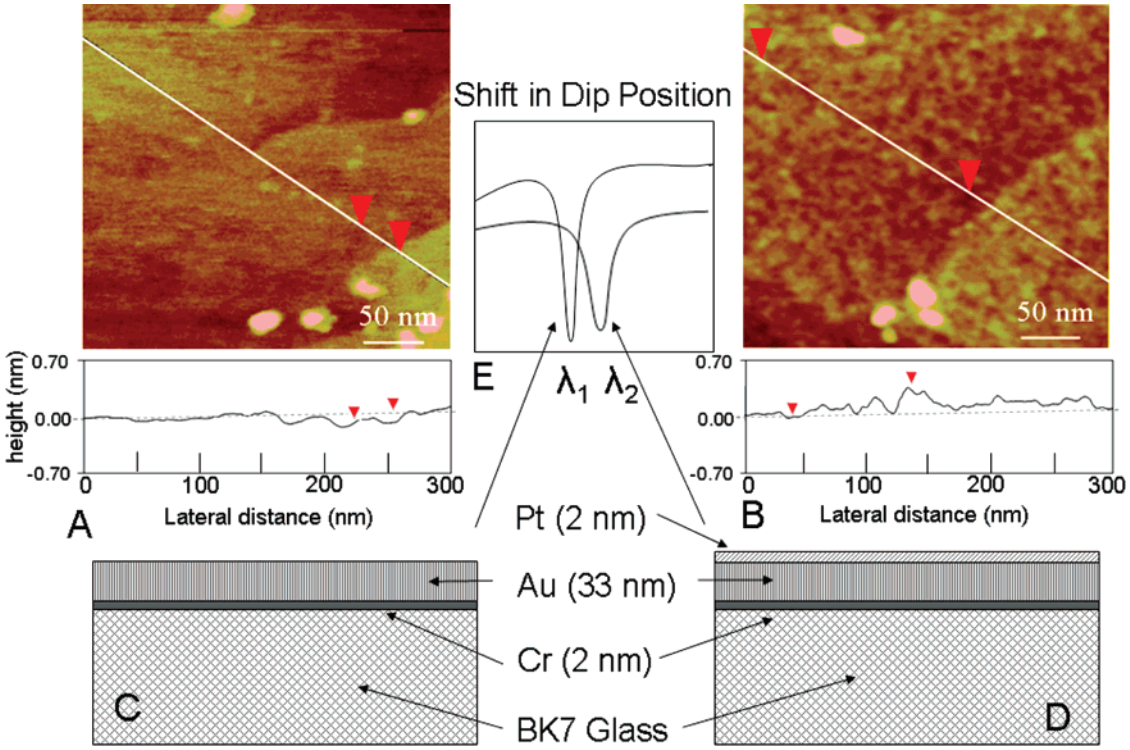

Figure 1. Atomic force microscopy images (A and B) from the Au and Pt surfaces, respectively, and schematics (C and D) of the layered substrates used for SPR analyses. The change in the reflectivity of the chip due to the 2-nm-thick platinum coating is shown in E and is compared to that from a bare gold surface. The insets are surface line profiles showing an rms roughness of less than 1 nm for each surface.

The Pt layer was deposited on the gold substrate, which resulted in a thin, continuous film on the surface. Because the film had to be extremely thin, it were characterized extensively to ensure continuity and uniform roughness (less than 1 nm) using the AFM. Continuous platinum films of similar thickness were previously achieved using the same system and characterized in a collaborative work.[28]

Besides providing quantitative utility of peptide interactions and adsorption on Pt surfaces, the approach also offers a novel method of studying such interactions between any molecule and a Pt substrate and also potentially offers the means to study the dynamics of chemical interactions (if these could produce a change in the index of refraction near the surface).

The SPR measurements were recorded at 27 ± 0.1 °C using a temperature controller system. The solutions used for the experiments flowed through the apparatus by means of a peristaltic pump (80 μL/min), and switching between different solutions was achieved via the use of a six-port valve (Upchurch Scientific). To establish a baseline for experimental measurements, solutions containing buffer alone were first flowed through the apparatus and coated slide. Next, buffer solutions containing each peptide (1, 2.5, 4, 7.5, 10, and 15 μg/mL final peptide concentrations) were introduced. After a specified interval to allow peptide adsorption onto the Pt thin films, a solution consisting of buffer minus peptide was allowed to flow through the system in order to monitor peptide desorption from the target thin film. The SPR data were collected using WinSpectral 1.03 software, which measures the normalized dip spectrum at periodic intervals (Figure 1). This dip is fitted to a fourth-degree polynomial function used to generate the time-dependent metric sensogram.[26]

Circular Dichroism (CD) Experiments. Lyophilized synthetic peptides were individually dissolved in distilled deionized water to create stock solutions. Each stock solution was then diluted to 30, 20, 15, 12, 9, and 6 μM for CD spectrometry measurements in 100 μM Tris HCl (pH 7.5). On the basis of the concentration variation studies, the optimal concentration was chosen to be 30 μM, and this concentration was utilized for further 2,2,2-trifluoroethanol (TFE, Acros Chemicals, 99.8%) titration studies (10, 30, 50, 70, and 90 vol %). All CD spectra were obtained at 25 °C with an AVIV 60 CD spectrometer running 60DS software (version 4.1t). The CD spectrometer was previously calibrated with d_{10}-camphorsulfonic acid. Wavelength scans were conducted from 185 to 260 nm with appropriate buffer and solvent background subtraction.[29,30] For each spectrum, three scans were averaged using a 1 nm bandwidth and a scanning rate of 0.5 nm/s. Mean residue ellipticity [θ_M] is expressed in deg·cm^2/dmol^{-1}.[31]

Molecular Modeling Studies. In the modeling studies, selected Pt binder sequences were either prepared in linear form or modified by the addition of cysteine residues at both N and C termini. Cysteine-modified peptides were then manually constrained with a disulfide bridge to mimic experimentally used constrained peptide libraries. The energy minimization of these peptides was carried out under vacuum conditions using the conformational analysis software provided with HyperChem molecular modeling software.[32] The conformational search module finds the minimum-energy points by varying the chosen dihedral angles. The software changes the dihederal angles randomly and creates new initial structures to perform energy minimization. In each round of energy minimization, unique low-energy conformations are stored, and high-energy and duplicate structures are discarded. Using the conformational search module, we found 1000 different local minima on the potential energy surface, and we chose the lowest one as the global minimum or the lowest-energy conformation.[21,33]

Results and Discussion

Using the M13 phage pIII tail constrained library, we originally selected Pt-binding sequences and, from this, identified strong binders. The PTSTGQA sequence possesses the highest affinity

(28) Allred, D. B.; Zin, M. T.; Ma, H.; Sarikaya, M.; Baneyx, F.; Jen, A. K.; Schwartz, D. T. *Thin Solid Films* **2007**, *515*, 5341−5347.
(29) Collino, S.; Kim, I. W.; Evans, J. S. *Cryst. Growth Des.* **2006**, *6*, 839−842.
(30) Kim, I. W.; Collino, S.; Morse, D. E.; Evans, J. S. *Cryst. Growth Des.* **2006**, *6*, 1078−1082.
(31) Evans, J. S. *Curr. Opin. Colloid Interface Sci.* **2003**, *8*, 48−54.
(32) *Hyperchem 7.5*; Hypercube Inc.: Gainesville, FL, 2003.
(33) Cubellis, M. V.; Caillez, F.; Blundell, T. L.; Lovell, S. C. *Proteins: Struct., Funct., Bioinf.* **2005**, *58*, 880−892.

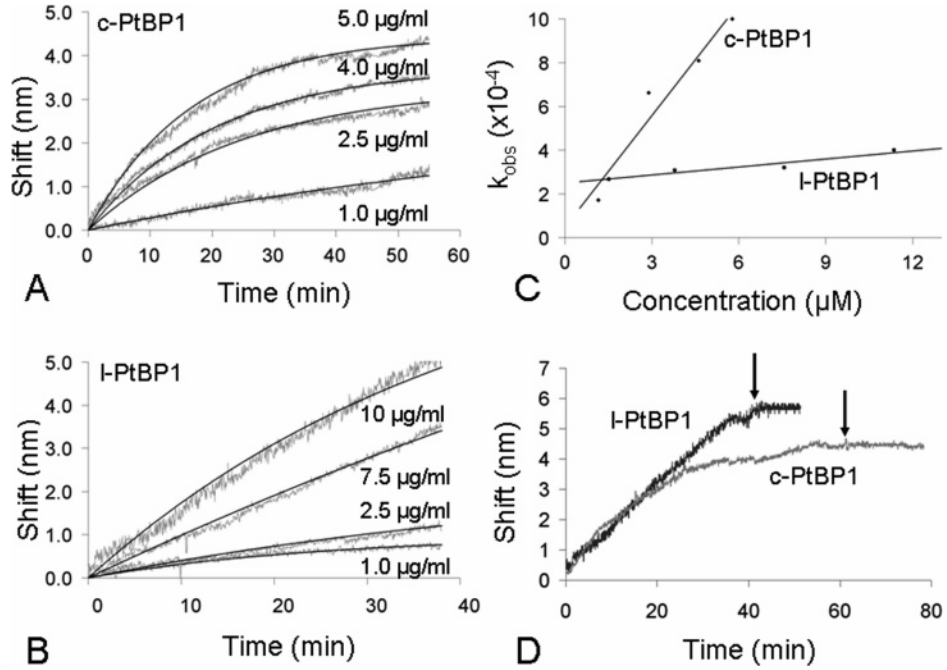

Figure 2. Adsorption isotherms for cyclic-PtBP1 (c-PtBP1) and linear-PtBP1 (l-PtBP1) (A and B, respectively) based on SPR measurements. Gray lines represent experimental data, and solid lines are Langmuir model fits. (C) Apparent adsorption rate coefficients, k_{obs}, plotted as a function of peptide concentration. Linear regression was performed to calculate the adsorption (k_a) and desorption (k_d) rates. (D) Adsorption/desorption behavior of the platinum-binding peptides from the surface of the SPR substrate during the rinse with the buffer. Neither of the peptides shows significant desorption on the time scale of the rinse phase, indicating a low desorption rate. Values of 10.0 and 5.0 μg/mL correspond to the maximum concentrations used in these experiments for linear and cyclic peptides, respectively.

Table 1. Adsorption Rate k_a, Desorption Rate k_d, Equilibrium Coefficient K_{eq}, and Free Energy for Linear (l) and Constrained (c) PtBP1 Peptides[a]

peptides	k_a^1 ($M^{-1}\,s^{-1}$)	k_a^2 ($M^{-1}\,s^{-1}$)	$k_d^1 \times 10^{-5}$ (s^{-1})	$k_d^2 \times 10^{-4}$ (s^{-1})	$K_{eq}^1 \times 10^6$ (M^{-1})	$K_{eq}^2 \times 10^4$ (M^{-1})	ΔG_{ads}^1 (kcal/mol)	ΔG_{ads}^2 (kcal/mol)
l-PtBP1	8.27 ± 0.92	10.2 ± 1.3	5.00 ± 0.57	3.00 ± 0.33	0.16 ± 0.04	3.39 ± 1.24	-7.16 ± 0.14	-6.22 ± 0.14
c-PtBP1	170 ± 3.44		5.00 ± 0.88		3.40 ± 0.89		-8.97 ± 0.13	

[a] The errors represent standard deviations.

for Pt as identified by immunofluorescence microscopy.[5,13] We utilized the SPR technique[23−27] to monitor the intermolecular interactions between the solid Pt thin film and the engineered peptide sequences both in cyclic and linear forms. To obtain the SPR signal used to monitor the molecular interaction with the solid surface, we constructed SPR substrates possessing a few-nanometers-thick platinum film on a Cr−Au-coated glass substrate. The data from these experiments were used to calculate the kinetic coefficients of the peptides, k_a and k_d (i.e., adsorption and desorption rate constants, respectively), and the equilibrium constant, K_{eq} (Table 1, Figure 2), using the appropriate Langmuir models (Supporting Information). As shown in Figure 2, the SPR data obtained for cyclic-PtBP1 fits the single 1:1 Langmuir model well. However, the data fit obtained for linear PtBP1 was found to fit a modified, biexponential Langmuir model[23] (Figure 2, Table 1), with two corresponding sets of k_a, k_d, and K_{eq} constants (Table 1). The major differences in adsorption kinetics indicate that the rate of adsorption of l-PtBP1 onto Pt is more complex than that of c-PtBP1.

The difference in adsorption is reflected in the rate and equilibrium constants obtained for both peptides. As shown in Table 1, we note that the k_a and K_{eq} values for cyclic peptides are nearly 20 times greater than those obtained for the linear form. Therefore, there is an approximately 2 kcal/mol difference in the Gibbs free energy of binding of cyclic versus linear peptides at room temperature. Here, we calculated the standard Gibbs free energy of adsorption as an approximation in describing the binding energy because the calculations are performed on the basis of the equilibrium constant rather than using the data that could be generated from the binding experiments at different temperatures.[23] However, the energy of adsorption found here is directly related to the free energy of the peptide; therefore, we refer to it as binding energy in the lieu of the free energy (Table 1). Collectively, these findings indicate that both cyclic-PtBP1 and linear-PtBP1 bind to Pt thin films but are kinetically different from each other with regard to adsorption behavior on a Pt substrate and that cyclic-PtBP1 is the higher-affinity binder of the two sequences.

Another interesting feature of the inorganic binding peptides is that the adsorption behavior of this group of molecules on a solid material surface is different than the conventional interactions usually studied between two biological molecules (e.g., one bound to a solid surface through a thiolate molecular linker and the other in solution as an analyte, where the binding affinity is dictated by the differences in adsorption and desorption rate constants of similar magnitudes). Here, in inorganic-binding peptides, a low desorption profile is observed, which is a desired characteristics for these peptides in molecular linker applications. Therefore, the adsorption process dominates in the control of the binding event. Also, in peptide adsorption onto a solid surface, there may be additional interactions involved compared to the well-known molecular interactions occurring in solution between molecules through recognition, resulting in a more complex peptide−solid binding process and causing variations in the

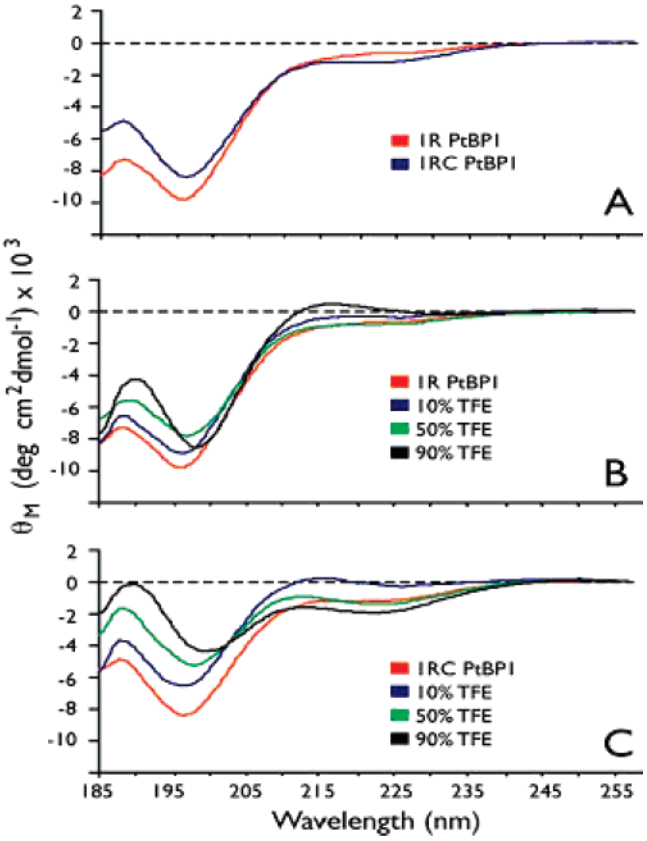

Figure 3. CD spectra of 30 μM linear-PtBP1 and cyclic-PtBP1 peptides (A) in 100 μM Tris HCl, pH 7.5 and (B and C) in the presence of varying volume percentages of TFE in 100 μM Tris HCl, pH 7.5.

Langmuir adsorption behavior. The additional processes may include surface diffusion, reorganization, and reconformation of the peptide and peptide−peptide interactions on the solid surface sometimes leading to supramolecular self-assembly of the peptide.[13]

Given the observed differences in adsorption rates, we were interested in learning if linear-PtBP1 and cyclic-PtBP1 differed with regard to internal structure as well. Specifically, we wanted to discover the effect that the Cys-Cys loop constraint might have on the secondary structure of the integral PtBP1 sequence. As shown in Figure 3A, the CD spectra for both peptides exhibit (−) $\pi-\pi^*$ transition bands centered at 197 nm, which is consistent with the presence of the random coil (RC) conformation in equilibrium with other secondary structures.[29,30] Hence, both the linear and cyclic forms exist as unfolded, structurally unstable species under aqueous conditions, a molecular feature that is common to other inorganic-binding peptide sequences.[29−31] However, upon closer examination, we note that a subtle structural difference exists between the two peptides. Specifically, linear 1-PtBP1 displays a weak n$-\pi^*$ ellipticity band centered at 200−225 nm. This band is more positive in ellipticity compared to the $\pi-\pi^*$ band associated with cyclic 1-PtBP1. The presence of a (+) ellipticity band in the 220−228 nm wavelength region is consistent with the presence of extended helical polyproline type II (PPII) secondary structure,[33−36] which has been noted in short peptides that contain Pro, Ala, and Gln.[35] Thus, although both peptides feature the same integral sequence and possess some degree of random coil, our findings indicate that the linear form of PtBP1 also adopts some degree of PPII structure in solution but the cyclic version does not.

Because PPII-forming amino acids[33−36] comprise the integral Pt binding sequence, we suspected that the cyclic-PtBP1 peptide does not readily adopt a PPII structure in solution because of the presence of the Cys-Cys loop constraint. To investigate this possibility, we performed CD experiments on both peptides in the presence of varying volume percentages of the structure-stabilizing solvent 2,2,2-trifluoroethanol (TFE, Figure 3B,C).[36] Here, we qualitatively evaluated the conformational stability as the response of each peptide to an external perturbation reagent.[36] For linear-PtBP1, we observe two phenomena: first, as a function of TFE content, the $\nu-\pi^*$ transition ellipticity band (218 nm) increases in (+) intensity, and second, the $\pi-\pi^*$ ellipticity band experiences a slight red shift to higher wavelength (200 nm). These spectral features are consistent with an increase in the percentage of PPII structure and the simultaneous loss of random coil structure, which indicates that TFE has an impact on the conformation of the linear-PtBP1 sequence.[36] This is not surprising because the linear form has unconstrained termini and should be responsive to alterations in solvent conditions. However, we observe slightly different conformational behavior for cyclic-PtBP1. At a low TFE percentage (10% v/v), we initially observe a (+) increase in the n$-\pi^*$ ellipticity band (218 nm), corresponding to an increase in PPII structure content. However, as the TFE content increases beyond 10% v/v, we note that a different structural fate is in store for the cyclic peptide. First, the $\pi-\pi^*$ ellipticity band shifts to higher wavelength (200 nm), indicating a shift in conformational equilibrium away from random coil secondary structure.[34−36] Second, the n$-\pi^*$ band becomes (−) in intensity and shifts to 222 nm, which is consistent with the presence of nonrandom coil structure, such as helix or beta turn.[29−31,36] The fact that an α-helix-associated ellipticity band at 208 nm is not observed suggests that the cyclic peptide cannot adopt a true α-helix structure under these conditions. Nonetheless, the cyclic-PtBP1 peptide cannot replicate the same TFE-induced conformational transition exhibited by linear-PtBP1. We interpret these results as follows: (a) Because each peptide possesses the same integral sequence (PTSTGQA) that consists of two PPII-forming amino acids, it is likely that the inherent secondary structure of the 7-AA sequence is a combination of RC and PPII. (b) However, in the presence of the covalent Cys-Cys loop, the cyclic version attempts to adopt a PPII structure (Figure 3), but it is frustrated in this endeavor by the presence of molecular constraint. Instead, the cyclic sequence adopts nonrandom and random coil structure in the presence of TFE to satisfy the existing molecular constraint of a covalent loop. This result experimentally verifies our earlier finding obtained through molecular modeling studies of the platinum-binding septapeptides, confirming that certain molecular architectures contain a multiple polypods lattice match with the platinum crystal surface.[21] The degree of binding might differ with the molecular architecture possessed by the peptide because of the availability of reactive side groups for surface interactions.

The conformational features discussed above may be further investigated by modeling studies presented in Figure 4. Here the molecular dynamic models provide more detailed analyses of the cyclic and linear peptides that have either a compact or an open form, respectively. The rigid form is a consequence of the constraint exerted on the septapeptide by the presence of the covalent C−C loop, resulting in a molecular architecture that is more rigid. Because of the absence of such structural constraints, the linear form of the peptide is more flexible with a high degree

(34) Kentsis, A.; Mezei, M.; Gindin, T.; Osman, R. *Proteins: Struct., Funct., Bioinf.* **2004**, *55*, 493−501.
(35) Chellgren, B. W.; Creamer, T. P. *Biochemistry* **2004**, *43*, 5864−5869.
(36) Kulp, J. L., III; Minamisawa, T.; Shiba, K.; Evans, J. S. *Langmuir* **2007**, *23*, 3857−3863.

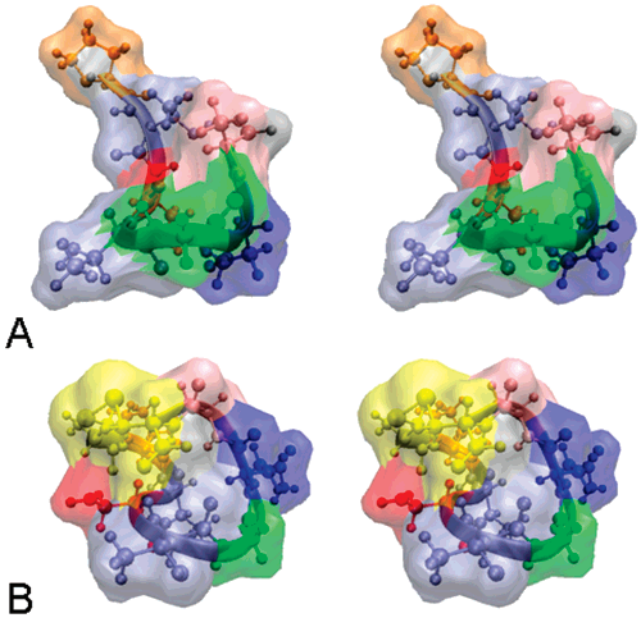

Figure 4. Pseudo-3D view (stereopairs) of molecular architectures of (A) linear-PtBP1 and (B) cyclic-PtBP1. The amino acids are colored as CPTSTGQAC.

of freedom in its conformation. We postulate, therefore, that the compact structure imposed by the Cys-Cys loop affects the motion, the binding dynamics, and the adsorption kinetics of the Pt-binding sequence. The linear form, because of its high degree of flexibility, is more floppy and therefore has slower adsorption behavior. Our present study provides compelling evidence that molecular features, such as a loop constraint, can exert significant influence on peptide adsorption onto inorganic materials such as Pt. The fact that linear-PtBP1 exhibits biexponential Langmuir adsorption behavior clearly suggests that the adsorption process for the linear form may involve an additional event or step that does not occur in the single Langmuir cyclic-PtBP1 adsorption process. This additional step may involve peptide conformational rearrangement or repositioning of the short 7-AA sequence on the Pt surface that occurs after the initial peptide binding event on Pt. If we assume that the short linear sequence has some degree of freedom or motion that permits this extra step in the adsorption process, then we conclude that this extra step or event may be prohibitive in the case of the cyclic-PtBP1 sequence as a result of the presence of the loop restraint and the corresponding loss of degrees of freedom.

The presence of a loop restraint also affects another important feature of these sequences, namely, secondary structure preferences and conformational stability. It is unusual that the integral 7-AA sequence possesses some degree of PPII conformation, a structure associated with protein intermolecular interactions with macromolecules.[34−36] However, we believe that the presence of the Cys-Cys loop leads to the destabilization of the PPII structure in favor of a different scenario: The random coil conformation in equilibrium with what appears to be an α-helix structure. It is likely that the restrained conformational and dynamic properties of cyclic-PtBP1 favorably modulate the binding of this peptide to Pt surfaces, possibly by altering the side-chain accessibility or positioning with respect to the target surface that leads to higher affinity interactions between cyclic-PtBP1 and Pt surfaces.

At this point, it is not clear whether Cys-Cys constrained M13 pIII phage sequences would be universally superior to linearized versions with regard to adsorption rates for a wide range of materials. However, we speculate that the presence or absence of the Cys-Cys loop restraint might be utilized to "tweak" the adsorption rate of a given material-specific peptide sequence, which, in turn, could be used as a building strategy in molecular engineering for biomimetic devices or hybrid materials involving peptides and inorganic solids. Obviously, additional experimentation will be required to ascertain this possibility. In conclusion, our work describes a quantitative interrogation of induced molecular structural characteristics of a new set of material-specific peptide sequences, explicitly to noble metal platinum, with respect to the dynamics of molecular binding. This report also demonstrates various ways of studying peptide interactions with solid surfaces, an understanding of which is essential in the robust utilization of this new class of engineered biomolecules as molecular linkers and as erectors in wide-ranging applications in bionanotechnology.[5,13]

Acknowledgment. This work was supported by grants from the National Science Foundation through the Genetically Engineered Materials Science & Engineering Center (GEMSEC), an MRSEC, the U.S. Army Research Office through the Defense University Research Initiative on NanoTechnology (DURINT) program, and the Turkish State Planning Organization via Advanced Technologies in Engineering (C.T.). Portions of this work represent contribution number 35 from the Laboratory for Chemical Physics, NYU (J.S.E.). We also thank Mr. C. So for technical help with AFM analyses.

Supporting Information Available: The experimental procedures for phage display, details of Langmuir adsorption isotherm calculations, and details of AFM experiments. This material is available free of charge via the Internet at http://pubs.acs.org.

LA700446G